USING THE ATTITUDE RESPONSE OF AEROSTABLE SPACECRAFT TO DETERMINE THERMOSPHERIC WIND

Josep Virgili-Llop

Naval Postgraduate School
Spacecraft Robotics Laboratory
700 Dyer Rd., Monterey CA 93940 USA

Peter C.E. Roberts and Zhou Hao

University of Manchester
School of Mechanical,
Aerospace and Civil Engineering
Sackville Street, Manchester, M13 9PL, UK

ABSTRACT

Thermospheric wind can be measured by observing the attitude motion of aerostable spacecraft when allowed to freely react to the aerodynamic torques. Estimates of the spacecraft aerodynamic properties, of the other disturbance torques and of the atmospheric density are required to determine the wind magnitude and direction. Aerostable spacecraft behave as undamped oscillators with their natural frequency depending on the dynamic pressure and their aerodynamic stiffness. The achievable spatial resolution is proportional to the natural frequency and smaller spacecraft, having higher cross-section area to inertia ratio, exhibit higher frequencies and are particularly suited for this method. The method described in this paper can provide global cross-track and in-track wind measurements. The measurements accuracy and spatial resolution with respect to the system parameters are analyzed and discussed for an ideal one rotational degree-of-freedom case.

Index Terms— thermospheric wind, estimation, spacecraft aerodynamics

1. INTRODUCTION

Wind is an important driver of thermosphere dynamics. Although it plays an important role in the electrodynamics of the upper atmosphere due to the ion/neutral interaction, there is not yet a good knowledge of the thermospheric wind, in part, due to the lack of measurements [1, 2].

There are multiple ways of measuring the thermospheric wind, using both in-situ and remote sensing techniques. In-situ measurements have been performed by spacecraft carrying sensitive accelerometers, which measure the accelerations caused by aerodynamic forces. Although these methods are only able to retrieve the cross-track component (crosswind) [3, 4, 5], they have been used successfully with data provided by the CHAMP, GRACE and GOCE accelerometers (and even using Mars Global Surveyor and Odyssey data on Mars [6]). Accelerometers based measurements are limited to crosswind because the acceleration measurement is also used to estimate the atmospheric density and to do so the in-track wind must be assumed (usually set to 0) [5]. If a different source of density data could be obtained (e.g. from a mass spectrometer) then in-track wind effects could be discriminated in the acceleration accelerometer data [7].

Of particular relevance to the accelerometer method is the work that has been recently conducted using CHAMP accelerometer data [1, 8, 9, 10, 11]. CHAMP wind measurements have a wind speed resolution of about ±10 m/s and a spatial resolution of 76 km [9]. Work from the GOCE datasets has also started to appear in the literature [12, 13]. The ongoing SWARM mission is also expected to yield thermospheric wind measurements [14].

Studying the atmosphere by observing the effects that aerodynamic forces have on the spacecraft dynamics has been done since Sputnik 1 [15]. By observing the change in the orbit inclination it can be deduced that the atmosphere co-rotates and that average west-east winds are of the order of 100 m/s. This was first done by observing how Sputnik 2 inclination decreased from its initial 65.33 to about 65.19 at the end of its life [16], and many more similar observations followed afterwards. Although the results of this type of analysis are too geographically and time averaged to be useful to advance atmospheric science, they are nonetheless important for orbital dynamics [17].

Sounding rockets have also been traditionally used to take in-situ measurements of the wind [18]. The technique employed releases a chemical tracer (usually sodium, lithium, and trimethyl aluminum) as the rocket ascends (or descends) through the layers of interest. The chemical tracers produce visible light and hence their motion can be tracked and the wind velocities inferred. Sodium and lithium produce resonant emissions that only occur when the vapor is illuminated. Therefore, measurements can be made when the trails are illuminated by the sun but the observers on the ground are in darkness (thus only viable at dusk or dawn). Trimethyl aluminum (TMA) on the other hand reacts on contact with oxygen to produce chemiluminescence, so observations at night are possible. Optical tracking of the trails provides wind pro-

files with good height resolution, in generally 0.5 km or better, and relatively small uncertainties, generally below 5 m/s [2]. As of 2002, approximately over 500 chemical tracer measurements have been made since 1958, with the vast majority at the 80 to 180 km altitude range [18, 2].

Remote sensing methods from ground-based or space-based instruments do also exist. These use either interferometer techniques or incoherent scatter radar techniques. On the interferometer front, Fabry–Prot Interferometers (FPI) are the most common instrument used and have been widely employed to measure the thermosphere winds both from space and from the ground. An FPI observes the Doppler shift of airglow emitted by different chemical species (mainly atomic oxygen) [19]. As the airglow emissions occur at an specific wavelength (e.g. at 6300 Å for O(^{1}D)) accurate Doppler measurements can be taken and thus the velocity of these particles inferred. It is not possible to obtain the three components of the wind simultaneously from a single measurement. Ground based instruments generally assume that the vertical component of the wind is small and then take measures at the four cardinal points (i.e. N-E-S-W) to obtain the overhead zonal and meridional components (by the difference between North-South and East-West measurements) [20]. If the instrument is well calibrated the vertical component can be obtained by taking a direct zenith measurement [20]. Multiple instruments observing the same location have been often used to obtain instantaneous zonal and meridional wind measurements [21]. Although FPI are the most common instrument used for the interferometer technique Michelson interferometers have also been used [22]. Ground based FPI have an uncertainty on their measurements of roughly $\sim$2-30 m/s [23, 24] (depending on the facility) during nighttime and $\sim$70 m/s during daytime [25]. According to [26] in 2006 there were less than 15 ground based FPIs over the entire world.

The NASA's Dynamic Explorer-2 (DE-2) launched in 1981 combined the results of its Fabry–Prot Interferometer (remote sensing) and its Wind and Temperature Spectrometer (in-situ) to obtain wind measurements [27]. With its polar orbit, the DE-2 FPI was capable of measuring the meridional winds (north–south direction) [28]. The Wind and Temperature Spectrometer measured the angle of arrival of the beam of neutral gas particles entering the spectrometer and thus it was capable of taking in-situ measurements of the zonal winds (west-east direction) [29]. Reliable wind measurements could only be made over the perigee part of the orbit. Due to the highly eccentric orbit only one polar region could be sampled during a given season [8].

Another spacecraft that has used the interferometer technique is the the Upper Atmosphere Research Satellite (UARS) [22]. On board this spacecraft was the Wind Imaging Interferometer (WINDII), which is a Michelson interferometer that measures Doppler shifts of the green line (557.7 nm) and red line (630.0 nm) airglow emissions at the Earth's limb. It had the capability of measuring the winds within the 80-300 km altitude range in a single image with an accuracy of about 1 km (limited by the stability of the UARS platform).

UARS also carried the High Resolution Doppler Imager (HRDI), a triple-etalon Fabry-Prot interferometer [30, 31]. Observing the emissions and adsorption lines of molecular oxygen it was capable of measuring the winds in small volumes (4 km in height by 50 km in width) at about 70–120 km altitude range with an accuracy of approximately 5 m/s.

The TIMED spacecraft had also a limb-scanning Fabry-Perot interferometer which is called TIMED Doppler Interferometer (TIDI) [32]. This instrument could measure daytime and nighttime winds at the 85-105 km altitude band and had a vertical resolution 2.5 km and with an accuracy that approaches $\sim$3 m/sec under optimum viewing conditions.

Measurements of thermospheric wind using incoherent scatter radar have been done for more than 20 years [33]. At the vicinity of Kiruna, in Sweden, the Incoherent scatter radar as the EISCAT (70N, 19E) has been operating for many years. In an ISR the wind is measured by the doppler shift in the signal scattered by the ionospheric plasma in the line of sight of the radar. EISCAT can measure the wind in a wide range of altitudes (from 180-360 km) and its results agree within 10 m/s from those obtained by WINDII [34, 35].

The method here proposed is conceptually similar to the in-situ measurements using spacecraft accelerometer data, but instead of measuring the linear acceleration it measures the angular accelerations. This technique, if used with another method to determine density, can obtain cross- and in-track wind measurements and thus can be used to complement or augment other in-situ measurements (such as accelerometer-based measurements).

First an overview of the proposed method is provided. Two different approaches are presented, an iterative based approach and a more simple frequency based. Both of these approaches are developed for a one degree-of-freedom case, but could be extended to a multidimensional case. Finally a case study is presented where, for an ideal case without uncertainties, the accuracy of the different approached is derived.

2. METHOD

By observing the attitude evolution of an uncontrolled aerostable spacecraft, the atmospheric wind can be measured. In this analysis, an aerostable spacecraft is defined as a vehicle which exhibits a restoring aerodynamic torque when it departs from its aerodynamic equilibrium attitude. Due to the high velocity of the relative flow, the effect of the spacecraft's angular velocity is negligible on the aerodynamic torque and thus the spacecraft will oscillate around the equilibrium attitude once perturbed. The aerodynamic torque can then be considered as conservative.

The variable atmospheric wind is one of the many perturbations affecting the aerostable spacecraft and thus the atti-

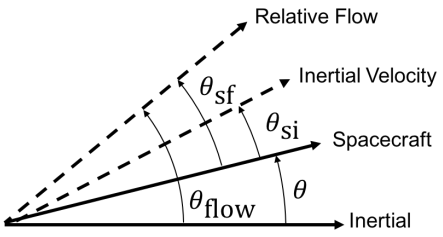

Fig. 1: Angle definitions.

tude evolution of the spacecraft will be affected by the wind making it observable. The challenge is to discern the wind effect from all the other perturbations.

In this analysis, a one rotational degree-of-freedom case will be considered, which will be capable to recover the meridional and zonal winds. The method can then be later extended to a multidimensional case and thus also recover the vertical winds (see section 4).

Let θ_{sf} denote the attitude of the spacecraft with respect to the relative flow and θ_{si} the attitude with respect the inertial velocity. The attitude with respect to the arbitrary inertial frame will be simply denoted by θ and the direction of the relative flow with respect to this inertial frame is denoted by $\theta_{\mathrm{f}low}$ and so $\theta - \theta_{\mathrm{sf}} = \theta_{\mathrm{flow}}$. An schematic definition of these different attitudes is shown in Fig. 1.

It is assumed that the θ_{si} attitude is known by the attitude determination subsystem (e.g. by using star-trackers and a GPS to determine the inertial velocity direction and magnitude). Additionally, the position of the spacecraft is also assumed to be known (e.g. by using a GPS receiver) and so the atmosphere co-rotation at that particular point can be easily computed and discounted. The attitude of the spacecraft with respect the combined inertial velocity and co-rotation θ_{sico} can then be derived and is also assumed to be known. The difference between the attitude with respect the incident relative flow θ_{sf} and the inertial velocity plus co-rotation θ_{sico} is only due to the atmospheric wind.

If only aerodynamic perturbations are considered the attitude motion is only a function of θ_{sf} and of the the relative flow magnitude $\|V_{\mathrm{f}}\|$. Conceptually the spacecraft will oscillate around the equilibrium point and the oscillation frequency is related to the relative flow magnitude. When other perturbations (e.g. residual magnetic dipole) are present, they will have to be estimated so that their attitude effect can be discounted when measuring the wind. To augment the signal to noise ratio it is clear that these other non-aerodynamic perturbations need to be as small as possible and thus spacecraft with a high degree of aerostability (i.e. with high restoring torques) are desirable.

2.1. Spacecraft Dynamics

In rarefied-gas aerodynamics the aerodynamic torques can be defined as in Eq. (1) [36].

$$\tau_{\mathrm{aero}} = \frac{1}{2}\rho V_{\mathrm{f}}^2 A_{ref} l_{ref} C_T \tag{1}$$

Where ρ denotes the atmospheric density, V_{f} the bulk velocity of the gas particles relative to the spacecraft and A_{ref}, l_{ref} are arbitrarily defined reference areas and lengths (usually tied to spacecraft dimensions). The C_T term, known as the torque coefficient, is a dimensionless coefficient that combines the spacecraft aerodynamic properties (shape and surface properties), flow properties (composition and temperature) and the orientation of the spacecraft with respect to the flow.

Assuming that all the spacecraft and flow parameters remain constant then C_T is only a function of the spacecraft attitude with respect to the flow $C_T\left(\theta_{\mathrm{sf}}\right)$. Note that the relative flow also includes the wind and hence its direction is not known a priory. It is also important to point that the relative flow velocity V is composed by the inertial velocity V_{i}, the atmospheric co-rotation velocity V_{co} and the wind velocity w and thus it is also initially unknown.

An aerostable spacecraft exhibits a restoring torque when its attitude is not aligned with the equilibrium one (making it statically stable). To simplify the notation, without loosing generality, it will be assumed that the equilibrium attitude is defined as $\theta_{\mathrm{sf}} = 0$.

In general, the restoring torque will not be linear with the angle deviation $\tau_{aero} = -qf\left(\theta_{\mathrm{sf}}\right)$, where the function $f\left(\theta_{\mathrm{sf}}\right)$ can be known by analyzing the aerodynamic properties of the spacecraft. To simplify the analysis it will be assumed that the restoring torque is proportional to the θ_{sf}. This assumption is generally valid for small angles of misalignment. With these assumptions, the restoring torque can be written, for a one-dimensional case as in Eq. (2) (where $q = 1/2\rho V^2$ denotes the dynamic pressure).

$$\tau_{\mathrm{aero}} = -qk\theta_{\mathrm{sf}} \tag{2}$$

With k denoting the aerodynamic stiffness, which takes into account the spacecraft aerodynamic properties (the relative flow bulk properties are contained in the dynamic pressure q). Note how an aerostable spacecraft with a linear restoring torque is analogous to a mass spring system. The spring stiffness equivalent is qk and the displacement equivalent is θ_{f}.

If the aerodynamic properties of the spacecraft (k or $f\left(\theta_f\right)$), the density ρ, inertial V_{i} and atmospheric co-rotation velocities V_{co}, and the aerodynamic torque τ_{aero} were known the direction of the relative flow θ_{sf} and its magnitude V_{f} could be computed using Eq. (2). As all the other magnitudes are known the wind direction and magnitude can then be immediately derived.

By observing the inertial attitude evolution, mainly the angular velocity $\dot{\theta}$ and angular acceleration $\ddot{\theta}$, the total torque τ_{tot} acting on a spacecraft can be computed by using the Euler equations as shown in Eq. (3). The known spacecraft inertia is denoted by I.

$$\tau_{\text{tot}} = I\ddot{\theta} + \dot{\theta} \times I\dot{\theta} \tag{3}$$

The total torque τ_{tot} does include the aerodynamic torque τ_{aero}, but also the gravity gradient τ_{grav}, the solar radiation pressure τ_{SRP}, the residual dipole τ_{mag} and the actuator's torque $\tau_{\text{actuators}}$ contributions as shown in Eq. (4).

$$\tau_{\text{tot}} = \tau_{\text{aero}} + \tau_{\text{grav}} + \tau_{\text{SRP}} + \tau_{\text{mag}} + \tau_{\text{actuators}} \tag{4}$$

By observing the inertial attitude evolution of the spacecraft θ, the angular velocity $\dot{\theta}$ and angular acceleration $\ddot{\theta}$ could be derived. Alternatively specific sensors for $\dot{\theta}$ and $\ddot{\theta}$ could be included in the spacecraft. The atmospheric density ρ also needs to be known and thus a specific sensor (e.g. mass spectrometer or accelerometer) is required.

The other torques acting on the spacecraft need to be known or at least, they need to be estimated before computing τ_{aero} (using Eq. (4)). Note that the bigger τ_{aero} is with respect to the other torques the less important the estimation accuracy of these other torques become, so a high τ_{aero} is desirable (effectively rising the signal to noise ratio). Thus a high aerodynamic stiffness k is desirable to achieve a high τ_{aero}.

Two different approaches to extract the wind measurements will be presented. The first one uses an iterative method where each wind component, in-track and cross-track are measured on different points, which are selected to have minimum sensitivity to the component that is not being measured at that point. These measurements are iteratively refined (interpolating the wind components). The second approach is simpler as the angular acceleration is not required during the estimation process. By measuring the frequency and the angle during the oscillation zero-crossing both wind components can be recovered.

2.2. Iterative approach

Considering a one-dimensional case significantly simplifies the analysis and notation while already showing which are main properties of the method. For simplicity, it will be also assumed that the restoring torque is linear (see Eq. (2)) and that aerodynamic torque τ_{aero} is the only torque applied to the spacecraft (no other perturbations considered). In such a simplified case, the governing equation can be expressed as Eq (5).

$$I\ddot{\theta} = -qk\theta_{\text{sf}} \tag{5}$$

Let the the wind w be represented by an in-track component w_i and a cross-track component w_c ($w^2 = w_i^2 + w_c^2$). The in-track component is aligned with the inertial velocity V_{i} direction and the cross-track component is perpendicular to it. The goal of the method is then to recover these two components of the wind. To simplify this case even further, without loosing generality, it will be assumed that the inertial velocity V_i is aligned with the inertial axes so when the spacecraft is aligned with the inertial velocity $\theta_{\text{i}} = 0 \rightarrow \theta = 0$. Additionally for this scenario it will be assumed that there is no atmospheric co-rotation (to make it general the atmospheric co-rotation can be included as part of the wind components). Under these assumptions, the dynamic pressure q and θ_{sf} or θ_{flow} can be written as follows.

$$q = \frac{1}{2}\rho\left(\left(V_i + w_i\right)^2 + w_c^2\right) \tag{6}$$

$$\tan\left(\theta - \theta_{\text{sf}}\right) = \tan\left(\theta_{\text{flow}}\right) = \frac{w_c}{V_i + w_i} \tag{7}$$

The magnitudes that are assumed to be known (or are assumed to be directly measured) are: spacecraft inertia I, aerodynamic stiffness k, atmospheric density ρ, inertial velocity V_i, spacecraft attitude θ, angular velocity $\dot{\theta}$ and acceleration $\ddot{\theta}$. At a single point in time the system can be reduced to a single equation (combining Eqs. (5), (6) and (8)) and thus both the in-track and cross-track can not be in principle measured simultaneously. In order to compute both components the dynamic behavior of the system needs to be inspected and some assumptions made.

As the restoring torque is linear the system is analogous to a forced mass-spring system and it will oscillate around it's equilibrium point. The natural frequency ω of this system can be easily computed using Eq. (8).

$$\omega = \sqrt{\frac{qk}{I}} \tag{8}$$

Although the final objective is to measure both the in-track and the cross-track wind components, it may be initially interesting to explore how the cross-track wind can be computed if the in-track wind component is ignored - set to zero - or known (previously estimated). A hat will be used to differentiate the estimated magnitudes from the known variables ($\hat{w}_i$ denotes the in-track wind estimation).

As the inertial velocity is generally much greater than the in-track wind $V_i > w_i$, initially assuming that $\hat{w}_i = 0$ will only introduce a small error in q and in θ_{flow}, after a more accurate estimation of the in-track wind is obtained the results can be updated (which forms the basis of the iterative approach). With this assumption, the cross-track component of the wind can be easily iteratively computed at any time during the oscillation using the simplified Eqs. (9)-(12) (by initially setting $\hat{w}_c = 0$ or another previously known estimate and updating this value until it converges). During the iterations the $\hat{w}_i$ will remain constant at a predefined value (e.g. $\hat{w}_i = 0$).

$$\hat{q} = \frac{1}{2}\rho\left((V_i + \hat{w}_i)^2 + \hat{w}_c^2\right) \tag{9}$$

$$\hat{\omega} = \sqrt{\frac{\hat{q}k}{I}} \tag{10}$$

$$\hat{\theta}_{flow} = \frac{\ddot{\theta}}{\hat{\omega}^2} + \theta \tag{11}$$

$$\hat{w}_c = (V_i + \hat{w}_i)\tan\left(\hat{\theta}_{flow}\right) \tag{12}$$

Obviously, this method converges to the true cross-track wind only if the estimate of the in-track wind $\hat{w}_i$ is completely accurate (which in general it will not be). As the system oscillates there will be times where the error introduced by an inaccurate in-track wind estimation $\hat{w}_i$ is smaller. The sensitivity of the estimated cross-track wind with respect to the in-track wind $\frac{\partial w_c}{\partial w_i}$ (shown in Eq. (13)) can offer a method to minimize this error.

$$\frac{\partial w_c}{\partial w_i} = \frac{w_c}{V_i + w_i} - \frac{2\ddot{\theta}}{\omega^2} \tag{13}$$

To minimize the error induced by an inaccurate $\hat{w}_i$ on $\hat{w}_c$, $\frac{\partial w_c}{\partial w_i}$ has to be minimized (as it shows how sensitive is the cross-track winds solution to an error in in-track wind estimate). During the attitude oscillations caused by the aerostability, where the angular acceleration $\ddot{\theta}$ also oscillates, there will be times where the sensitivity is larger than others. The measurements are to be taken when this sensitivity is at its minimum and resulting in the most accurate cross-track wind estimate possible. Achieving a $\frac{\partial w_c}{\partial w_i} = 0$ completely eliminates the error associated with an inaccurate in-track estimate as in the measurement of the cross-track component is insensitive - independent - from the in-track estimate. This conditions is achieved at a certain angular acceleration level as shown in Eq. (14).

$$\ddot{\theta} = \frac{\omega^2 w_c}{2\left(V_i + w_i\right)} \approx \frac{\omega^2 w_c}{2V_i} \tag{14}$$

Unfortunately, this point of zero sensitivity depends on the in-track component and thus it will not be accurately known, but as $V_i \gg w_i$ the Eq. (14) approximation will not be very far from the ideal location. It is also important to note that the point where to take the measurements is also dependent on the cross-track component w_c which is the magnitude to be measured and thus initially unknown.

To solve this situation the cross-track component will be continuously estimated during the oscillation and there will be certain points where Eq. (14) is satisfied and thus the estimates associated with those locations are the ones presenting a smaller error. It is important to note that this minimum sensitivity condition occurs twice every oscillation and thus two good cross-track measurement per oscillation can be taken.

As at this point good estimates of the cross-track components are available and a similar procedure can be used to estimated the in-track component $\hat{w}_i$. By iteratively using using Eqs. (15)-(18) with previously obtained estimates of the cross-track wind $\hat{w}_c$ an estimate of the in-track wind $\hat{w}_i$ can be obtained.

$$\hat{\theta}_{\text{flow}} = \arctan\left(\frac{\hat{w_c}}{V_i + \hat{w_i}}\right) \tag{15}$$

$$\hat{\omega}^2 = \frac{\ddot{\theta}}{\hat{\theta}_{\text{flow}} - \theta} \tag{16}$$

$$\hat{q} = \frac{\hat{\omega}^2 I}{k} \tag{17}$$

$$\hat{w_i} = \sqrt{\frac{2\hat{q}}{\rho} - \hat{w_c^2}} - V_i \tag{18}$$

Again, as this set of equations assumes a certain cross-track component (which in general will not be completely accurate), an error will be introduced when estimating $\hat{w}_i$. To minimize it, the measurements can be taken when $\frac{\partial w_i}{\partial w_c}$ is minimum. It is easy to see that from Eq. (13) that $\frac{\partial w_i}{\partial w_c}$ will be minimum when $\left\|\ddot{\theta}\right\|$ is maximum. In this case the error will not be completely eliminated as $\frac{\partial w_i}{\partial w_c}$ will not cross through zero. It is also important too note that maximum acceleration is achieved twice per oscillation and thus two good measurements per oscillation of the in-track component are available.

With these two iterative processes, the cross-track and in-track wind components can be estimated. As the measurement point of of the in-track and cross-track components is not coincident the estimates need to be interpolated so they are available when obtaining the other wind component estimates (i.e. cross-track wind interpolation is required to obtain the cross-track estimate used when estimating the in-track component). The spacecraft data can be first collected to be later processed as no real-time estimation is required. The iterative process is then repeated multiple times subsequently refining the estimates and updating the interpolation.

2.3. Frequency approach

Measuring the frequency of the oscillation provides an alternative approach to measure the winds. If it is assumed that the wind components are averaged over an oscillation (denoted by $\bar{w_c}$ and $\bar{w_i}$), and substituting the dynamic pressure (Eq. (6)) and θ_{flow} into the equation of motion results in the following Eq. (19).

$$I\ddot{\theta} = -\frac{1}{2}\rho\left[(V_i + \bar{w_i})^2 + \bar{w_c}\right]k\left(\theta - \arctan\left(\frac{\bar{w_c}}{V_i + \bar{w_i}}\right)\right) \tag{19}$$

Similarly the natural frequency can be written as follows.

$$\omega = \sqrt{\frac{\rho}{2I}\left[(V_i + \bar{w}_i)^2 + \bar{w}_c^2\right]} \tag{20}$$

Eqs. (19) and (20) can be solved to obtain the averaged wind values over the oscillation. Firstly obtaining the in-track wind and cross-track wind from the natural frequency results in the following expressions.

$$\bar{w}_i = \sqrt{\left(\frac{2I\omega^2}{\rho k} - \bar{w}_c^2\right)} - V_i \tag{21}$$

$$\bar{w}_c = \sqrt{\frac{2I\omega^2}{\rho k} - (V_i - \bar{w}_i)^2} \tag{22}$$

Substituting the solution for $\bar{w}_i$ into the equation of motion gives the following expression.

$$\ddot{\theta} = -\omega^2 \left(\theta - \arctan\left(\sqrt{\frac{\bar{w}_c^2}{\frac{2I\omega^2}{\rho k} - \bar{w}_c^2}}\right)\right) \tag{23}$$

Then, solving for $\bar{w}_c$ gives the following expression that provides the cross-track wind based on the current angle, angular acceleration and oscillation frequency.

$$\bar{w}_c = \sqrt{\frac{2I\omega^2}{\rho k}\sin^2\left(\frac{\ddot{\theta}}{\omega^2} + \theta\right)} \tag{24}$$

Following the same procedure for $\bar{w}_i$ yields the following equation to determine in-track wind.

$$\bar{w}_i = \sqrt{\frac{2I\omega^2}{\rho k}\cos^2\left(\frac{\ddot{\theta}}{\omega^2} + \theta\right)} - V_i \tag{25}$$

With these equations, one could imagine a scheme where measurements are taken four times per oscillation. Two measurements are taken when the angular rate is maximum $\dot{\theta}_{\max}$ (where $\theta_{\dot{\theta}\max} = \theta_{\text{flow}}$ and $\ddot{\theta}_{\dot{\theta}\max} = 0$). In that case Eqs. (24) and (25) can be written as follows (remembering that $\tau = 2\pi/\omega$).

$$\bar{w}_c = \sin\left(\theta_{\dot{\theta}\max}\right)\frac{2\pi}{\tau}\sqrt{\frac{2I}{\rho k}} \tag{26}$$

$$\bar{w}_i = \cos\left(\theta_{\dot{\theta}\max}\right)\frac{2\pi}{\tau}\sqrt{\frac{2I}{\rho k}} - V_i \tag{27}$$

Another two measurements are taken when there is maximum angular acceleration $\ddot{\theta}_{\max}$ (where the angular amplitude with respect to the flow θ_{sfmax} is maximum). In this case the equations can be written as follows.

$$\hat{\bar{w}}_c = \sin\left(\frac{\ddot{\theta}_{\max}\tau^2}{4\pi^2} + \theta_{\max}\right)\frac{2\pi}{\tau}\sqrt{\frac{2I}{\rho k}} \tag{28}$$

$$\hat{\bar{w}}_i = \cos\left(\frac{\ddot{\theta}_{\max}\tau^2}{4\pi^2} + \theta_{\max}\right)\frac{2\pi}{\tau}\sqrt{\frac{2I}{\rho k}} - V_i \tag{29}$$

Note how the oscillation period is required to obtain the averaged estimates. The period can be easily obtain as four times the time between the maximum acceleration and maximum rate.

This other approach is not iterative and thus does not require previous knowledge of the in-track or cross-track wind. Also if the measurements are done when maximum rate is achieved (Eqs. (26) and (27)) there is no need to estimate angular acceleration, simplifying the whole measurement process and being potentially more accurate (an advantage over the iterative approach presented in section 2.2). This will then become the default option and thus two measurements per cycle will be obtained.

Unfortunately the assumption that the winds remain constant is quite limiting as the accuracy of the method can be significantly degraded if the winds variability is not well below the natural frequency of the spacecraft.

2.4. Spatial Resolution

If the wind is roughly constant and the spacecraft exhibits the aerodynamic aerostable response shown in Eq. (2) then the spacecraft will oscillate around its equilibrium point and thus, two measurements of in-track and two measurements of cross-track wind will be available per spacecraft oscillation (sampling frequency is 2ω). Using the Nyquist criterion it is easy to see that this method can recover wind frequencies that are lower than the oscillation frequency of the spacecraft (Eq. (8)).

This approach matches the results obtained if the transmissibility of the system is analyzed. As the spacecraft behaves as an undamped oscillator the only excitations (i.e. wind) that have an effect on the spacecraft attitude are those with a natural frequency around or below the spacecraft natural frequency. The transmissibility gain G with respect to the excitation frequency ω_w to natural frequency ratio ω_0 is shown in Fig. 2. This behavior helps to filter out wind variability that will be below the measurement frequency threshold (reducing errors) but also makes clear that to achieve an uncontrolled bounded oscillation the wind main frequency shall be below the spacecraft's natural frequency (to avoid the high gain region). The expected wind variability frequency can be coarsely estimated with current atmospheric models [37, 38, 12].

As the spacecraft is traveling across the atmosphere at a significant velocity, the temporal sampling frequency has an equivalent spatial resolution d. Equation (30) shows how the spatial resolution can be computed (or estimated if the effect of wind and atmospheric co-rotation on the natural frequency is ignored).

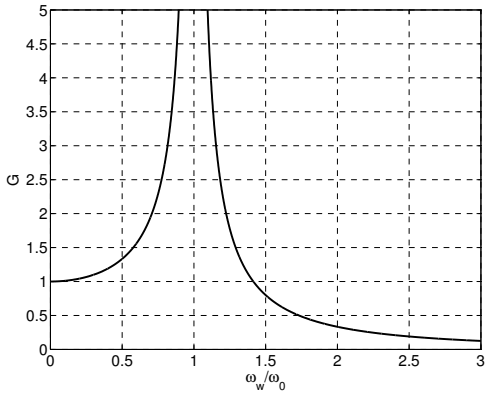

Fig. 2: Transmissibility gain for an undamped oscillator.

Table 1: ΔDsat properties.

Property	Value
Inertia in yaw	$I_z = 0.0318$ kg/m^2
Aerodynamic stiffness	$k = 0.17$ Nm/rad

$$d = \frac{2\pi V_i}{\omega} \approx 2\pi\sqrt{\frac{2I}{\rho k}} \tag{30}$$

The inertia I and, to a high degree, the aerodynamic stiffness k are only a function of the spacecraft mass and shape. As expected, low inertia spacecraft with high aerodynamic stiffness (exhibiting higher natural frequencies) will achieve a better spatial resolution. The atmospheric density has a significant effect on the spatial resolution. As the density exponentially increases with reduced altitudes the spatial resolution will exponentially improve with lowering altitudes.

3. CASE STUDY

To illustrate the proposed method a one-dimensional example is provided. The proposed prototype 2U ΔDsat CubeSat [39], which has been designed with the objective to recover atmospheric winds (see Fig. 3), will be used in this example.

This nanosatellite is expected to operate in an attitude that is roughly aligned with the relative flow. The long appendages located towards the trailing side of the spacecraft provide a large aerodynamic stiffness. The aerostable spacecraft is able to keep an oscillating attitude when left uncontrolled and thus no control torques are required during the measurement campaigns. The expected properties of this vehicle are provided in Table 1.

It will also be assumed that the spacecraft operates in keplerian circular orbit. The atmospheric density has been estimated using the NRLMSISE-00 model[40] with moderate solar activity[41].

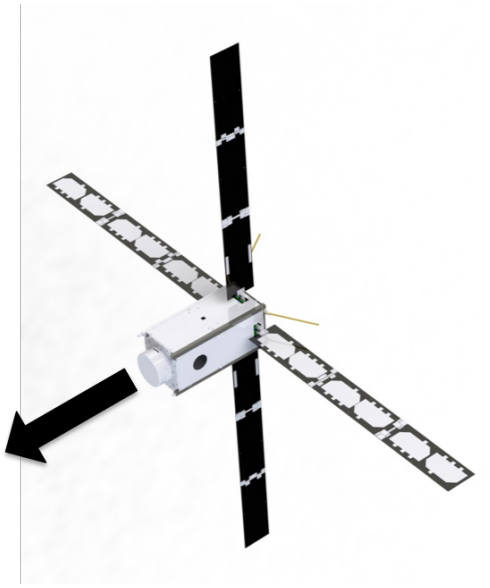

Fig. 3: External configuration of the proposed ΔDsat CubeSat.

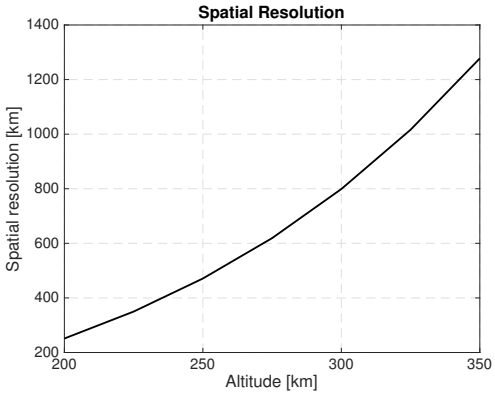

Fig. 4: Theoretical spatial resolution of the proposed ΔDsat CubeSat.

For this specific prototype design the theoretical spatial resolution with respect to the operating altitude is shown in Fig 4 (assuming a mean density).

Figure 5 shows the estimation errors for the iterative approach. A 200 m/s cross-track and in-track wind for different in-track and cross-track relative frequencies (relative to the spacecraft's natural frequency) has been used and it has perfect knowledge of the parameters and atmospheric conditions has been assumed. The attitude sampling frequency has been set to 1 Hz

It is clear from Fig. 5 that the cross-track wind can be estimated with very small uncertainties (below 5 m/s) at all frequencies. Much higher uncertainties are observed for the in-track wind (potentially limiting its usability). As expected, in both cases, as the wind frequencies approach the spacecraft

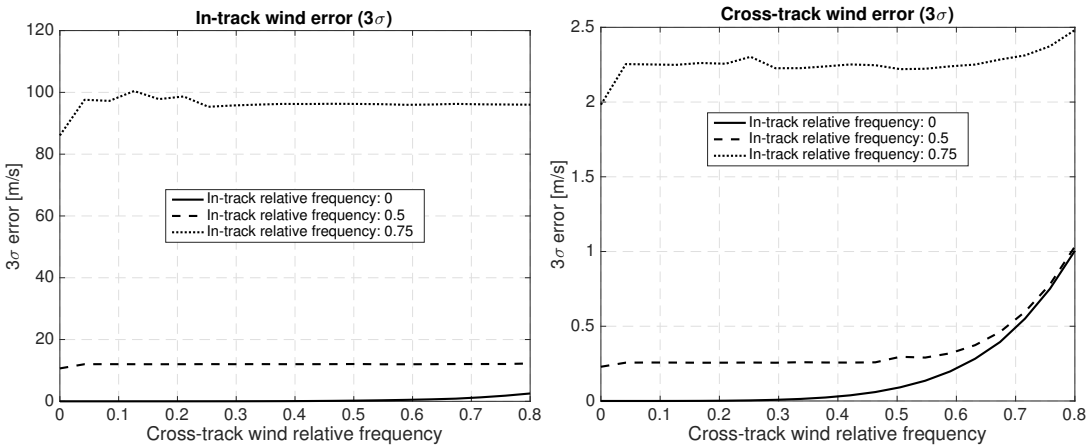

(a) (b)

Fig. 5: Error on in-track (a) and cross-track (b) wind estimation for the iterative approach.

natural frequency the uncertainties grow.

Figure 6 shows the estimation errors for the frequency approach using the same conditions. The frequency approach is more sensitive to timing errors and thus the attitude sampling frequency has been increased to 10 Hz.

4. MULTI-DIMENSIONAL CASE

Up to this point, a one-dimensional case has been derived. This allows to extract the zonal and meridional winds but leaves away the vertical winds. Although the vertical winds are generally smaller [13] it may interesting to recover them.

The method presented here can be easily extended for a multidimensional case. In a full three-dimensional case the full Euler equations need to be used (see Eq. (3)). In addition, the expression of the aerodynamic torque will be more complex $\tau_{\text{aero}} = f\left(\theta_{\text{flow}}\right)$ and thus an iterative numeric scheme to find θ_{flow} (as in a least-square) may be used. Then the winds that create the observed θ_{flow} can be determined. As in the one-dimensional case, there will be locations where the measurement error will be minimized.

5. CONCLUSION

The method presented can recover cross-track and wind-track winds by observing the attitude evolution of an aerostable spacecraft if the aerodynamic properties and the atmospheric density are known. This method could help complement the current accelerometers missions or be used as a standalone method if another type of density sensor is present. The main benefit of this method is that it needs to observe attitude evolution and in general accurate attitude sensors (i.e. star-trackers) are commercially available, in contrast with high-precision accelerometers as the ones included in GOCE. The main drawback of the method is that it needs a good characterization of the aerodynamic properties and that it requires a separate source of atmospheric density measurements.

6. REFERENCES

[1] K. Häusler, H. Lühr, S. Rentz, and W. Köhler, "A statistical analysis of longitudinal dependences of upper thermospheric zonal winds at dip equator latitudes derived from champ," *Journal of Atmospheric and Solar-Terrestrial Physics*, vol. 69, no. 12, pp. 1419–1430, 8 2007.

[2] M. F. Larsen and C. G. Fesen, "Accuracy issues of the existing thermospheric wind models: can we rely on them in seeking solutions to wind-driven problems?," *Annales Geophysicae*, vol. 27, no. 6, pp. 2277–2284, 2009.

[3] Huixin Liu, Hermann Lühr, Shigeto Watanabe, Wolfgang Köhler, Vance Henize, and Pieter Visser, "Zonal winds in the equatorial upper thermosphere: Decomposing the solar flux, geomagnetic activity, and seasonal dependencies," *Journal of Geophysical Research: Space Physics*, vol. 111, no. A7, pp. n/a–n/a, 2006.

[4] Eric K. Sutton, R. Steven Nerem, and Jeffrey M. Forbes, "Density and winds in the thermosphere deduced from accelerometer data," *Journal of Spacecraft and Rockets*, vol. 44, no. 6, pp. 1210–1219, 2007.

[5] Eelco Doornbos, Jose Van Den Ijssel, Hermann Luehr, Matthias Foerster, and Georg Koppenwallner, "Neutral density and crosswind determination from arbitrarily oriented multiaxis accelerometers on satellites," *Journal of Spacecraft and Rockets*, vol. 47, no. 4, pp. 580–589, 2015/02/27 2010.

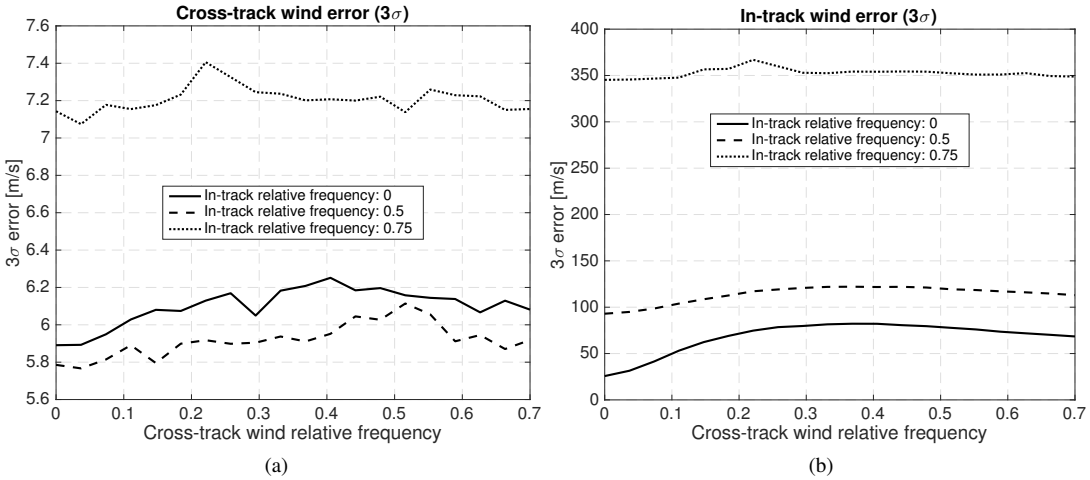

Fig. 6: Error on in-track (a) and cross-track (b) wind estimation for the frequency approach.

[6] Geoffrey Crowley and Robert Tolson, *Mars Thermospheric Winds from MGS and Odyssey Accelerometers*, American Institute of Aeronautics and Astronautics, 2015/03/21 2006.

[7] Kenneth Moe and Mildred Moe, *Method for Deriving Densities and In-Track Winds During Storms*, American Institute of Aeronautics and Astronautics, 2015/03/21 2006.

[8] H. Lühr, S. Rentz, P. Ritter, H. Liu, and K. Häusler, "Average thermospheric wind patterns over the polar regions, as observed by champ," *Annales Geophysicae*, vol. 25, no. 5, pp. 1093–1101, 2007.

[9] P. Ritter, H. Lühr, and E. Doornbos, "Substorm-related thermospheric density and wind disturbances derived from champ observations," *Annales Geophysicae*, vol. 28, no. 6, pp. 1207–1220, 2010.

[10] R. S. Lieberman, R. A. Akmaev, T. J. Fuller-Rowell, and E. Doornbos, "Thermospheric zonal mean winds and tides revealed by champ," *Geophysical Research Letters*, vol. 40, no. 10, pp. 2439–2443, 2013.

[11] W.T. Sivla and H. McCreadie, "Mid-latitude thermospheric zonal winds during the equinoxes," *Advances in Space Research*, vol. 54, no. 3, pp. 499 – 508, 2014, Recent Advances in Equatorial, Low- and Mid-Latitude Mesosphere, Thermosphere-Ionosphere System Studies.

[12] Douglas P. Drob, John T. Emmert, John W. Meriwether, Jonathan J. Makela, Eelco Doornbos, Mark Conde, Gonzalo Hernandez, John Noto, Katherine A. Zawdie, Sarah E. McDonald, Joe D. Huba, and Jeff H. Klenzing, "An update to the horizontal wind model (hwm): The quiet time thermosphere," *Earth and Space Science*, vol. 2, no. 7, pp. 301–319, 2015, 2014EA000089.

[13] S. Bruinsma S. Fritsche G. Koppenwallner P. Visser J. van den IJssel Doornbos, E. and J. de Teixeira de Encarnacao, "Goce+ theme 3:air density and wind retrieval using goce data final report," Tech. Rep. Tech. Rep. 4000102847/NL/EL, TU Delft, Netherlands, 2014.

[14] Pieter Visser, Eelco Doornbos, Jose van den IJssel, and João Teixeira da Encarnação, "Thermospheric density and wind retrieval from swarm observations," *Earth, Planets and Space*, vol. 65, no. 11, pp. 1319–1331, 2013.

[15] D.G. King-Hele, "The upper atmosphere as sensed by satellite orbits," *Planetary and Space Science*, vol. 40, no. 2–3, pp. 223 – 233, 1992.

[16] R. H. MERSON, D. G. KING-HELE, and R. N. A. PLIMMER, "Changes in the inclination of satellite orbits to the equator," *Nature*, vol. 183, no. 4656, pp. 239–240, 01 1959.

[17] D.G. King-Hele and Doreen M.C. Walker, "Upper-atmosphere zonal winds from satellite orbit analysis: An update," *Planetary and Space Science*, vol. 36, no. 11, pp. 1085 – 1093, 1988.

[18] M. F. Larsen, "Winds and shears in the mesosphere and lower thermosphere: Results from four decades of chemical release wind measurements," *Journal of Geophysical Research: Space Physics*, vol. 107, no. A8, pp. SIA 28–1–SIA 28–14, 2002.

[19] Gordon G Shepherd, *Spectral imaging of the atmosphere*, vol. 82, Academic press, 2002.

[20] C.A. Tepley, R.G. Burnside, J.W. Meriwether Jr., P.B. Hays, and L.L. Cogger, "Spatial mapping of the thermospheric neutral wind field," *Planetary and Space Science*, vol. 32, no. 4, pp. 493 – 501, 1984.

[21] Jonathan J. Makela, Daniel J. Fisher, John W. Meriwether, Ricardo A. Buriti, and Amauri F. Medeiros, "Near-continual ground-based nighttime observations of thermospheric neutral winds and temperatures over equatorial brazil from 2009 to 2012," *Journal of Atmospheric and Solar-Terrestrial Physics*, vol. 103, no. 0, pp. 94 – 102, 2013, Recent Advances in Equatorial, Low- and Mid-latitude Aeronomy.

[22] G. G. Shepherd, G. Thuillier, Y.-M. Cho, M.-L. Duboin, W. F. J. Evans, W. A. Gault, C. Hersom, D. J. W. Kendall, C. Lathuillère, R. P. Lowe, I. C. McDade, Y. J. Rochon, M. G. Shepherd, B. H. Solheim, D.-Y. Wang, and W. E. Ward, "The Wind Imaging Interferometer (WINDII) on the Upper Atmosphere Research Satellite: A 20 year perspective," *Reviews of Geophysics*, vol. 50, no. 2, pp. n/a–n/a, 2012.

[23] B. G. Fejer, J. T. Emmert, and D. P. Sipler, "Climatology and storm time dependence of nighttime thermospheric neutral winds over millstone hill," *Journal of Geophysical Research: Space Physics*, vol. 107, no. A5, pp. SIA 3–1–SIA 3–9, 2002.

[24] Q. Wu, D. McEwen, W. Guo, R.J. Niciejewski, R.G. Roble, and Y.-I. Won, "Long-term thermospheric neutral wind observations over the northern polar cap," *Journal of Atmospheric and Solar-Terrestrial Physics*, vol. 70, no. 16, pp. 2014 – 2030, 2008.

[25] A. J. Gerrard and J. W. Meriwether, "Initial daytime and nighttime sofdi observations of thermospheric winds from fabry-perot doppler shift measurements of the 630-nm oi line-shape profile," *Annales Geophysicae*, vol. 29, no. 9, pp. 1529–1536, 2011.

[26] J.W. Meriwether, "Studies of thermospheric dynamics with a fabry–perot interferometer network: A review," *Journal of Atmospheric and Solar-Terrestrial Physics*, vol. 68, no. 13, pp. 1576 – 1589, 2006, Passive Optics Aeronomy Passive Optics Workshop.

[27] T. L. Killeen, P. B. Hays, N. W. Spencer, and L. E. Wharton, "Neutral winds in the polar thermosphere as measured from dynamics explorer," *Geophysical Research Letters*, vol. 9, no. 9, pp. 957–960, 1982.

[28] P. B. Hays, T. L. Killeen, and B. C. Kennedy, "The Fabry-Perot Interferometer on Dynamics Explorer," *Space Science Instrumentation*, vol. 5, pp. 395–416, Dec. 1981.

[29] N. W. Spencer, L. E. Wharton, H. B. Niemann, A. E. Hedin, G. R. Carrignan, and J. C. Maurer, "The Dynamics Explorer Wind and Temperature Spectrometer," *Space Science Instrumentation*, vol. 5, pp. 417–428, Dec. 1981.

[30] Paul B. Hays, Vincent J. Abreu, Michael E. Dobbs, David A. Gell, Heinz J. Grassl, and Wilbert R. Skinner, "The high-resolution doppler imager on the upper atmosphere research satellite," *Journal of Geophysical Research: Atmospheres*, vol. 98, no. D6, pp. 10713–10723, 1993.

[31] M. D. Burrage, N. Arvin, W. R. Skinner, and P. B. Hays, "Observations of the o2 atmospheric band nightglow by the high resolution doppler imager," *Journal of Geophysical Research: Space Physics*, vol. 99, no. A8, pp. 15017–15023, 1994.

[32] T. L. Killeen, Q. Wu, S. C. Solomon, D. A. Ortland, W. R. Skinner, R. J. Niciejewski, and D. A. Gell, "Timed doppler interferometer: Overview and recent results," *Journal of Geophysical Research: Space Physics*, vol. 111, no. A10, pp. n/a–n/a, 2006.

[33] J. E. Salah and J. M. Holt, "Midlatitude thermospheric winds from incoherent scatter radar and theory," *Radio Science*, vol. 9, no. 2, pp. 301–313, 1974.

[34] C. Lathuillère, J. Lilensten, W. Gault, and G. Thuillier, "Meridional wind in the auroral thermosphere: Results from eiscat and windii-o(1d) coordinated measurements," *Journal of Geophysical Research: Space Physics*, vol. 102, no. A3, pp. 4487–4492, 1997.

[35] O. Witasse, J. Lilensten, C. Lathuillere, and B. Pibaret, "Meridional thermospheric neutral wind at high latitude over a full solar cycle," *Annales Geophysicae*, vol. 16, no. 10, pp. 1400–1409, 1998.

[36] David Mostaza Prieto, Benjamin P. Graziano, and Peter C.E. Roberts, "Spacecraft drag modelling," *Progress in Aerospace Sciences*, vol. 64, pp. 56 – 65, 2014.

[37] A. E. Hedin, E. L. Fleming, A. H. Manson, F. J. Schmidlin, S. K. Avery, R. R. Clark, S. J. Franke, G. J. Fraser, T. Tsuda, F. Vial, and R. A. Vincent, "Empirical wind model for the middle and lower atmosphere.," *Journal of Atmospheric and Terrestrial Physics*, vol. 58, no. 13, pp. 1421–1447, 1996.

[38] D. P. Drob, J. T. Emmert, G. Crowley, J. M. Picone, G. G. Shepherd, W. Skinner, P. Hays, R. J. Niciejewski, M. Larsen, C. Y. She, J. W. Meriwether, G. Hernandez, M. J. Jarvis, D. P. Sipler, C. A. Tepley, M. S. O'Brien, J. R. Bowman, Q. Wu, Y. Murayama, S. Kawamura, I. M. Reid, and R. A. Vincent and, "An empirical

model of the Earth's horizontal wind fields: HWM07," *Journal of Geophysical Research: Space Physics*, vol. 113, no. A12304, 2008.

[39] Josep Virgili and Peter C.E. Roberts, "DDsat, a QB50 CubeSat mission to study rarefied-gas drag modelling," *Acta Astronautica*, vol. 89, no. 0, pp. 130 – 138, 2013.

[40] J. M. Picone, A. E. Hedin, D. P. Drob, and A. C. Aikin, "NRLMSISE-00 empirical model of the atmosphere: Statistical comparisons and scientific issues," *Journal of Geophysical Research: Space Physics*, vol. 107, no. A12, 2002.

[41] ISO 14222, "ISO 14222 space environment (natural and artificial). Earth upper atmosphere," Tech. Rep. ISO 14222:2013, ISO, September 2013.